Transactions on the Built Environment vol 9, © 1995 WIT Press, www.witpress.com, ISSN 1743-3509

Finite element grid resolution based on second and fourth-order truncation error analysis

S.C. Hagen, J.J. Westerink
Department of Civil Engineering and Geological Sciences, University of Notre Dame, Notre Dame, Indiana 46556, USA

Abstract

Presently, many numerical modelers use the inadequate wavelength to grid size (Δx) ratio criterion as an aid in designing grids to solve the shallow water equations. Recent research has shown that grids designed using a local truncation error analysis (LTEA) are a very attractive alternative to the wavelength to Δx criterion. By computing grid spacing such that the local second-order truncation error is limited, we have shown the need for high resolution in areas on the continental shelf very near the coast and in the vicinity of the shelf break and slope.

This paper will examine the effects of combining the first through the fourth-order truncation error terms. Here the finite element grid generation is accomplished by computing grid spacing such that the local truncation error is limited. Our analysis shows that the inclusion of the first through the fourth-order truncation errors has a dramatic effect on the allowable grid size throughout our idealized one-dimensional (1-D) domain. We show the variable grid generated using truncation error analysis to be highly accurate in capturing the physics of our idealized 1-D domain. We reaffirm that the wavelength to Δx criterion is insufficient.

Introduction

Coastal hydrodynamic models are including larger domains and increasing levels of localized detail. The Western North Atlantic Tidal (WNAT) model domain, Figure 1, provides an explicit example of just how large domain sizes have grown [Westerink et al[1]; Blain et al[2]]. This domain size is justified when one considers the simplicity of open ocean boundary conditions on deep ocean boundaries for both tide and storm surge computations. The total area, 8.347×10^6 km^2, coupled with the need for near shore detail indicates the use of a finite element based model.

Generating a finite element grid for such large domains is typically accomplished using an inadequate criterion, namely the one-dimensional (1-D), linear, frictionless, constant topography wavelength to grid size ratio. This ratio is computed as:

$$\frac{\lambda}{\Delta x} = \frac{\sqrt{gh}}{\Delta x}T \tag{1}$$

Transactions on the Built Environment vol 9, © 1995 WIT Press, www.witpress.com, ISSN 1743-3509

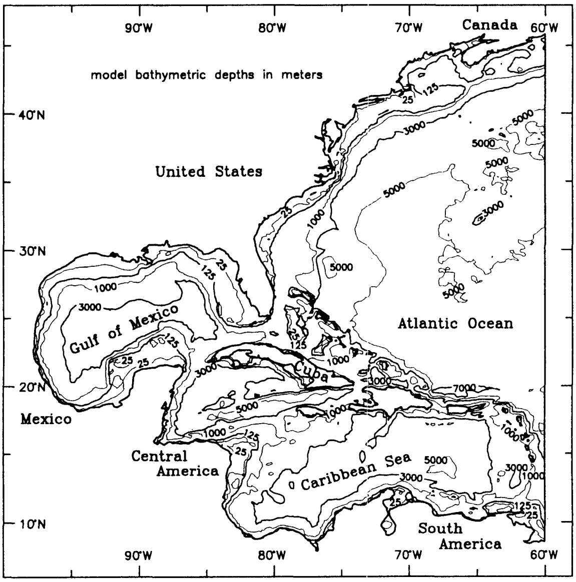

Figure 1: The WNAT model domain including bathymetry (in meters).

(where g = gravitational constant, h = water depth and T = tidal period). We have found, and will reaffirm in this paper, that this criterion will not lead to satisfactory graded grids. Presently, there is no dependable numerical basis for mesh generation which incorporates physics into the finite element grid generation process.

Our previous work, e.g. Hagen and Westerink[3], has shown that second-order local truncation error analysis (LTEA) can provide a reliable framework for finite element grid generation. With this paper we will present results from a first through fourth-order one-dimensional LTEA. The information that we gain from this detailed analysis of the first four terms of the truncation error series is shown to provide a workable finite element mesh generation routine which can be solely based on a second and fourth-order LTEA (which simplifies the procedure by excluding the first and third, or odd, ordered terms). 1-D grids generated using this routine will be shown to be highly accurate and extremely efficient.

Model Formulation

The computations in this paper were realized with a one-dimensional, finite element model of the linearized shallow water equations. The governing equations are formulated in the generalized wave continuity equation (GWCE) form [Lynch and Gray[4]; Kinnmark[5]; Luettich et al[6]]: the GWCE;

$$\frac{\partial^2 \eta}{\partial t^2} + \tau_0 \frac{\partial \eta}{\partial t} - g\frac{\partial}{\partial x}\left(h\frac{\partial \eta}{\partial x}\right) - (\tau - \tau_0)\frac{\partial}{\partial x}(uh) = 0 \qquad (2)$$

and the non-conservative momentum equation;

$$\frac{\partial u}{\partial t} + g\frac{\partial \eta}{\partial x} + \tau u = 0 \qquad (3)$$

Transactions on the Built Environment vol 9, © 1995 WIT Press, www.witpress.com, ISSN 1743-3509

(where t = time, η = the deviation of the free surface from the geoid, u = velocity in the x-direction, τ_0 = a weighting parameter in the GWCE, g = gravitational acceleration, h = depth relative to the geoid and τ = bottom friction coefficient). The spatial discretization of these equations is based on a standard Galerkin method and linear finite elements. Time is resolved using a three level weighted implicit finite difference approximation for the GWCE and a Crank Nicholson scheme for the momentum equation. Results were harmonically analyzed for both the elevation and velocity amplitudes and phases.

Bathymetric Representation

A bathymetric representation of a typical slice of the continental shelf, slope and rise of the Western Atlantic Ocean was constructed and is shown in Figure 2. Note that the ordinate is exaggerated nearly one hundred times. Of particular importance is the grade of the continental slope (2-degrees) and the location of the continental shelf break. Also note the locations of the toe of the continental rise and slope. The depth at the shoreline is 20 meters.

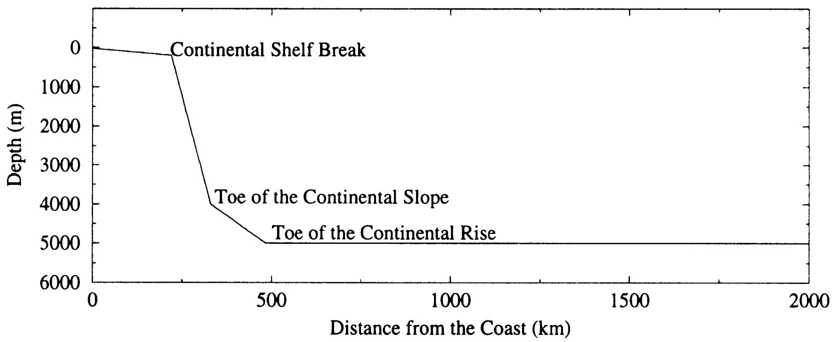

Figure 2: 1-D idealized bathymetry for LTEA.

Convergence Study

A very fine mesh (Δx = 1 km) is required to produce a truth solution for calculating the truncation errors and verifying results attained with a variable grid. Convergence for our truth solution was verified by comparing results of simulations using the 1 km regular mesh (2001 nodes; R1), a 0.5 km regular mesh (4001 nodes; R.5) and a 0.25 km regular mesh (8001 nodes; R.25). The level of convergence obtained with the 1 km regular mesh leads us to describe it as our "truth" grid.

Truncation Error Development

We now develop the truncation error for the one-dimensional, linear, harmonic shallow water equations. We obtain the harmonic form of the governing equations by substituting into equations (2) and (3), $u = \hat{u}e^{i\omega t}$ and $\eta = \hat{\eta}e^{i\omega t}$ (where $\hat{u}$, $\hat{\eta}$ = the complex amplitudes of u and η, $i = \sqrt{-1}$ and ω = the M_2 frequency). The harmonic form of the GWCE is written as (assuming that $\tau = \tau_0$):

$$-\omega^2\hat{\eta} + i\omega\tau_0\hat{\eta} - g\frac{\partial}{\partial x}\left(h\frac{\partial\hat{\eta}}{\partial x}\right) = 0 \qquad (4)$$

and the non-conservative momentum equation is expressed in harmonic form as:

$$i\omega\hat{u} + g\frac{\partial\hat{\eta}}{\partial x} + \tau\hat{u} = 0. \tag{5}$$

Applying the finite element method to these equations results in a discrete form of these equations. A typical interior node, j, representation of the linear, harmonic momentum equation is:

$$\frac{i\omega+\tau}{6}(\hat{u}_{j-1} + 4\hat{u}_j + \hat{u}_{j+1}) + \frac{g}{2\Delta x}(-\hat{\eta}_{j-1} + \hat{\eta}_{j+1}) = 0. \tag{6}$$

The nodal values of the variables are then approximated with Taylor Series expanded about node j, orders are separated and the continuous form, equation (5), is subtracted. What remains is the truncation error in series form. The first through the fourth-order terms in the truncation error series for the linear, harmonic form of the non-conservative momentum equation are expressed as:

$$\tau_{ME} = \frac{i\omega+\tau}{6}\left[2(\Delta x_{j+1} - \Delta x_j)\frac{\partial\hat{u}_j}{\partial x} + \left(\frac{\Delta x_j^3 + \Delta x_{j+1}^3}{\Delta x_j + \Delta x_{j+1}}\right)\frac{\partial^2\hat{u}_j}{\partial x^2} + \right. \tag{7}$$

$$\left. + \frac{1}{3}(\Delta x_{j+1} - \Delta x_j)\left(\Delta x_j^2 + \Delta x_{j+1}^2\right)\frac{\partial^3\hat{u}_j}{\partial x^3} + \frac{1}{12}\left(\frac{\Delta x_j^5 + \Delta x_{j+1}^5}{\Delta x_j + \Delta x_{j+1}}\right)\frac{\partial^4\hat{u}_j}{\partial x^4}\right] +$$

$$+ \frac{g}{6}\left[3(\Delta x_{j+1} - \Delta x_j)\frac{\partial^2\hat{\eta}_j}{\partial x^2} + \left(\frac{\Delta x_j^3 + \Delta x_{j+1}^3}{\Delta x_j + \Delta x_{j+1}}\right)\frac{\partial^3\hat{\eta}_j}{\partial x^3} + \right.$$

$$\left. + \frac{1}{4}(\Delta x_{j+1} - \Delta x_j)\left(\Delta x_j^2 + \Delta x_{j+1}^2\right)\frac{\partial^4\hat{\eta}_j}{\partial x^4} + \frac{1}{20}\left(\frac{\Delta x_j^5 + \Delta x_{j+1}^5}{\Delta x_j + \Delta x_{j+1}}\right)\frac{\partial^5\hat{\eta}_j}{\partial x^5}\right] + \text{H.O.T.}$$

where Δx_{j+1} and Δx_j indicate the inter-nodal spacing to the right and to the left of the node where the local truncation error is being estimated.

Note that when $\Delta x_{j+1} = \Delta x_j$ the odd-ordered truncation errors will cancel out. Therefore, in order to estimate the complete series of local truncation errors, one must have a graded finite element grid.

Evaluation of the Truncation Errors

Values for the truncation errors may be computed if one has an acceptable value to approximate the spatial derivatives of $\hat{u}$ and $\hat{\eta}$ at points throughout a given domain. We accomplished this by using the harmonically decomposed truth solution obtained with the 1 km grid to estimate the second and second and fourth-order truncation errors at each of the nodes. The first through the fourth-order local truncation errors are estimated by using the harmonically decomposed solutions obtained with a graded grid.

Transactions on the Built Environment vol 9, © 1995 WIT Press, www.witpress.com, ISSN 1743-3509

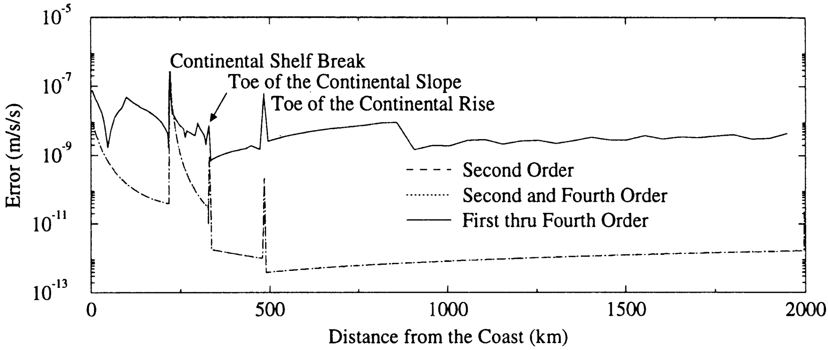

Figure 3: Local truncation error for the 1-D momentum equation.

The graded grid used for this LTEA was based on a second and fourth-order LTEA. Thus the estimation of the first through the fourth-order local truncation errors requires a second round of the LTEA process. Local truncation errors resulting from the non-conservative momentum equation were computed using fourth-order accurate finite difference approximations for the derivatives. The resulting local truncation error values are shown in Figure 3.

Much useful information can be gained by closely examining these local truncation errors. First we note that these errors are low and that we are doing a fine job of capturing the continuous equations. However, the spikes that are present indicate where the level of resolution leads to locally higher truncation errors, or alternatively where we may relax the level of resolution (which is the basis of these truncation error estimates). In order to obtain a workable grid we will relax the level of resolution and force the localized truncation error to be an approximately constant value throughout the domain. We use the truncation error information from the truth grid to effectively generate a variably spaced grid.

Note that the second and second and fourth-order local truncation errors fall on the same curve. The values of these two sets of local truncation errors are not exactly equal. And, the response to the various sets of local truncation errors varies widely (as we will see when node spacing requirements are presented in the next section).

Figure 3 also contains the first through fourth-order local truncation error curve. These errors are estimated by using a variably graded grid which is based on second and fourth-order local truncation errors. We can see a flattening out of the local truncation errors as the nodes are more strategically placed.

Grid Generation

By relaxing the grid size in regions where the truncation error is low, we can construct a grid with a more uniform distribution of truncation error as compared to the 1 km grid. Our approach is to accept that the truncation error at the continental shelf break is sufficiently low. We then use this value for the truncation error at each and every node and solve for the spacing which is required to maintain this value of the truncation error. Figure 4 presents a plot of the required spacings throughout the one-dimensional domain, based on the respective local truncation error analysis, using the maximum truncation error (2.81 E-07 m/s^2) from the one-dimensional momentum equation.

By including more of the truncation error terms in our LTEA, we influence the node spacing requirements and provide much useful information. First, previous work

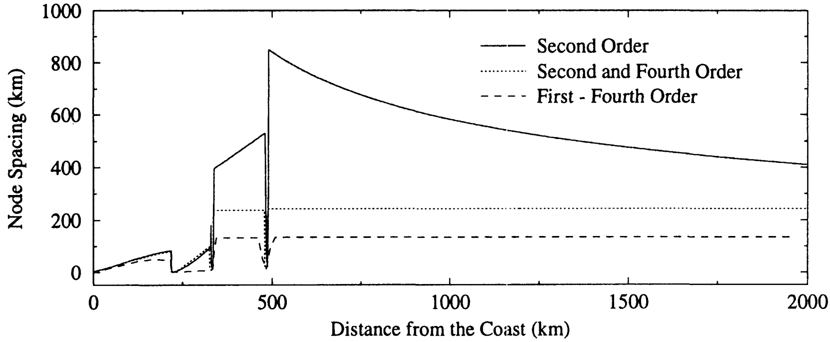

Figure 4: Required Δx based on LTEA of the 1-D momentum equation.

regarding the resolution requirements for deep ocean modeling has shown that an upper limit on Δx of 80 km is reasonable, e.g. Luettich and Westerink[7]. As more of the leading truncation error terms are included in the LTEA, deep ocean node spacing requirements approach this limit. Also, resolution on the continental rise, slope and shelf is increased. This also agrees with Luettich and Westerink[7].

One of the critical discoveries as a result of this LTEA are the observed multiple of change requirements. That is, we can see in Figure 4 that in most areas the required node spacing increases or decreases at a regular ratio. Focusing on the continental slope, we see that as we progress from left to right the node spacing requirements which are based on the second and second and fourth-order LTEA increase at a rate of 1.4 times the previous size. When we examine the node spacing requirements which are based on the first through fourth-order LTEA that rate of increase is 1.1 and it is enforced from right to left also.

The major obstacle left, in applying LTEA as a finite element grid generating scheme, is the realization that this method initially requires a highly resolved grid. This is fine when working in 1-D, but would prove to be computationally prohibitive in 2-D. Thus we have taken the following course. We estimate the second and fourth-order local truncation errors with a regular spaced coarse grid, Δx = 20 km, and generate the required node spacing based on that LTEA. We then adjust all local spacings so that the minimum spacing at the shelf break is equal to 1 km and enforce a maximum increasing multiple of change of 1.2 and a multiple of change of 1/1.2 when the node spacing is decreasing in size. Aside from the multiple of change requirement, which is after all

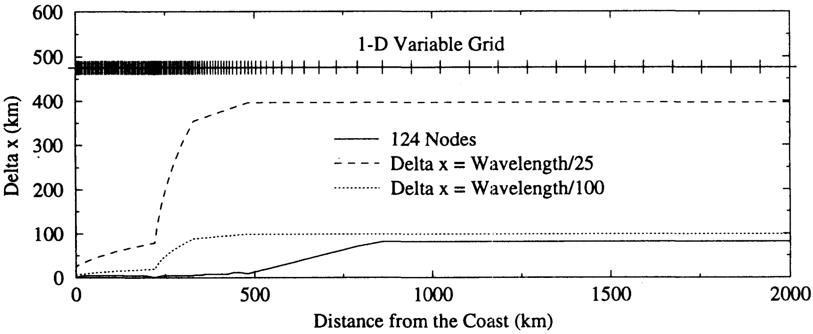

Figure 5: Variable 1-D grid based on LTEA and Δx using the wavelength to Δx ratio.

a product of the detailed first through fourth-order LTEA, the 124 node variable grid in Figure 5 is based solely on a second and fourth-order LTEA.

Figure 5 also contains plots of the spacing requirements if the wavelength to Δx ratio criterion were used. Two examples are plotted: when the wavelength to Δx ratio criterion is set to 25 and 100. Note that an increase in the wavelength to Δx ratio criterion from 25 to 100 improves the resolution at the extremes of our domain, that is in the deep ocean and the near-shore shallow water areas. However, the continental rise, slope and shelf break areas, while improved, are not being properly resolved. Obviously this is a result of the absence of physics when finite element grid generation is based on this 1-D, linear, frictionless, constant topography wavelength to grid size ratio.

LTEA does incorporate physics into the finite element grid generation process and proves to be highly accurate and efficient as we shall show in the next section.

Grid Verification

The computed errors for the 124 node variable grid, shown in Figures 6 and 7, indicate that this grid performs extremely well. A harmonic analysis was performed on the results of the 124 node variable grid and comparisons are made to the harmonically analyzed 1 km regular grid results. Figure 6 shows percent errors of the elevation and velocity amplitudes normalized by the "truth" amplitudes and Figure 7 presents the absolute elevation and velocity phases as compared with the "truth" phases. Our greatest errors occur with the velocity amplitudes. However, the percentage velocity error is held under 1% within nearly the entire interior of the one-dimensional domain. The

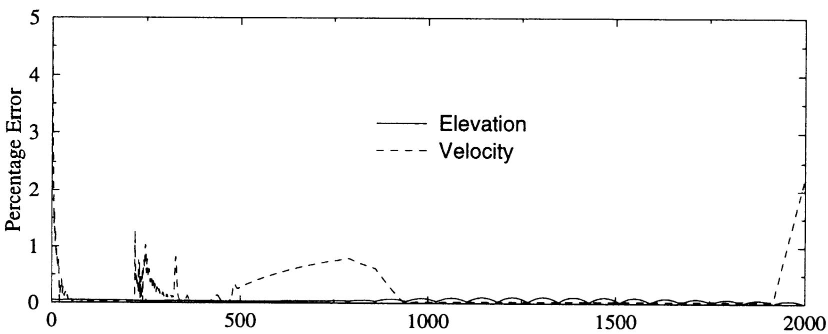

Figure 6: Percent elevation and velocity amplitude errors.

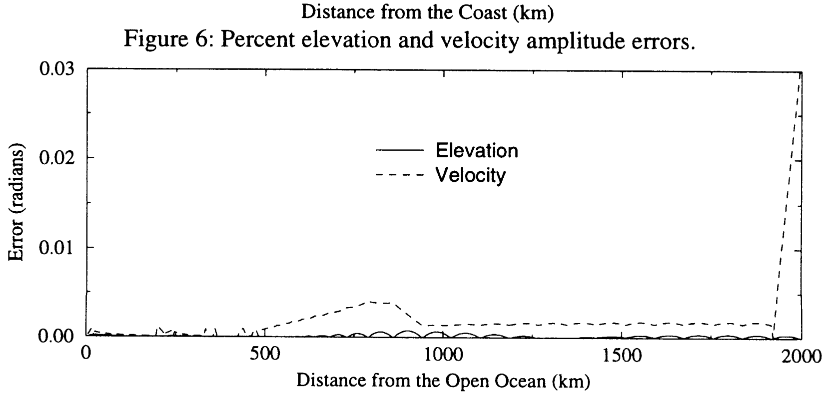

Figure 7: Absolute elevation and velocity phase errors.

higher (relatively) errors which occur on the boundaries can be attributed to the simplified boundary treatment and the elimination of the interior domain governing equations at the boundaries in favor of boundary equations.

Finally we present cpu time requirements on a Sun Sparc Station 20/50. When the truth grid with 2001 nodes was used, the cpu required 9770 seconds. The variable grid with 124 nodes performed the same simulation with only 575 seconds of cpu time (less than 6% of the time).

Conclusions

We draw five conclusions as a result of this research. First that LTEA provides a basis for finite element grid generation. Second, if the multiple of change is kept limited, we don't need to explicitly consider odd-order truncation terms. Third, that this method may be applied in an efficient manner which has good potential for 2-D grids (local truncation errors can be estimated with a coarse grid). Fourth, resolution in the area of the continental shelf break is critical. And finally, the wavelength to Δx ratio criterion is inadequate.

Acknowledgments

This research was supported by the U.S. Army Engineers Waterways Experiment Station under contract DACW-39-90-K-0021 and through a fellowship by the U.S. Department of Education through the GAANNP Program.

References

1. Westerink, J.J., Luettich, R.A. and Muccino, J.C., Modeling Tides in the Western North Atlantic Using Unstructured Graded Grids, *Tellus*, 1994, **46A**, 178-199.
2. Blain, C.A., Westerink, J.J. and Luettich, R.A., The Influence of Domain Size on the Response Characteristics of a Hurricane Storm Surge Model, *J. of Geophysical Research*, 1994, **99**, **C9**, 18,467-18,479.
3. Hagen, S.C., Westerink, J.J., Finite Element Grids Based on Truncation Error Analysis (ed CHES and IRTCES), pp. 2194 to 2201, Proceedings of the Second International Conference on Hydro-Science and -Engineering, Beijing, China, 1995.
4. Lynch, D.R. and Gray, W.G., A Wave Equation Model for Finite Element Tidal Computations, *Computational Fluids*, 1979, **7**, 207-228.
5. Kinnmark, I.P.E., *The Shallow Water Wave Equations: Formulation, Analysis and Application*, Ph.D. Dissertation, Dept. of Civil Eng., Princeton University, N. J., 1984.
6. Luettich, R.A., Westerink, J.J. and Scheffner, N.W., ADCIRC: An Advanced Three-Dimensional Circulation Model for Shelves, Coasts and Estuaries, Report 1: Theory and Methodology of ADCIRC-2DDI and ADCIRC-3DL, *Tech. Report DRP-92-6,* Department of the Army, 1992.
7. Luettich, R.A. and Westerink, J.J., Continental Shelf Scale Convergence Studies with a Barotropic Tidal Model, *Quantitative Skill Assessment for Coastal Ocean Models*, ed D.R. Lynch and A.M. Davies, A.G.U., 1994, In Press.